

UK/01-04
Aug. 2001

Chiral Properties of Pseudoscalar Mesons on a Quenched 20^4 Lattice with Overlap Fermions

S.J. Dong^a, T. Draper^a, I. Horváth^a, F.X. Lee^{b,c}, K.F. Liu^a, and J.B. Zhang^d

^a*Dept. of Physics and Astronomy, University of Kentucky, Lexington, KY 40506*

^b*Center for Nuclear Studies, Dept. of Physics, George Washington University, Washington, DC 20052*

^c*Jefferson Lab, 12000 Jefferson Avenue, Newport News, VA 23606*

^d*CSSM and Dep. of Physics and Math. Physics, University of Adelaide, Adelaide, SA 5005, Australia*

Abstract

The chiral properties of the pseudoscalar mesons are studied numerically on a quenched 20^4 lattice with the overlap fermion. We elucidate the role of the zero modes in the meson propagators, particularly that of the pseudoscalar meson. The non-perturbative renormalization constant Z_A is determined from the axial Ward identity and the pion decay constants f_π is calculated from which we determine the lattice spacing to be 0.157 fm.. We look for quenched chiral log in the pseudoscalar decay constants and the pseudocalar masses for both equal and unequal quark masses. We find that, given limited statistics, it is difficult to see quenched logs in pseudocalar masses with equal or unequal quark masses. Whereas, it is relatively clear to see them in the pseudoscalar matrix element and the ratio of the pseudoscalar matrix element to f_π . The chiral log parameter δ turns out to be consistent with that predicted from quenched chiral perturbative theory.

PACS numbers: 11.15.Ha, 12.28.Gc, 11.30.Rd

1 Introduction

One of the main goals of lattice QCD is to understand low-energy phenomenology as a consequence of chiral symmetry from first principles. Recent advances in the formulation of chiral fermions on the lattice hold great promise for studying the chiral symmetry of QCD at finite lattice spacing [1].

Neuberger's overlap fermion [2], derived from the overlap formalism [3], is such a chiral fermion on the lattice and has been implemented numerically to study chiral condensate [4, 5, 6], quark mass [7], renormalization constants [7, 8], short-distance current correlators [9], as well as to check chiral symmetry [7, 10] and scaling [7]. However these studies are limited to small volumes due to the large numerical cost associated with approximating the matrix sign function. In this paper, we shall study the physical observables, such as the hadron masses and pion decay constants close to the physical u, d quark mass. As such, we need to work on a lattice which is at least 3 times larger than the Compton wavelength of the pion with the smallest mass in order to alleviate finite volume effects. We work on a 20^4 lattice with $a = 0.157$ fm as determined from the pion decay constant f_π . This gives the lattice size $La = 3.14$ fm and the smallest pion mass is ~ 200 MeV. Thus, the lattice size is ~ 3 times the Compton wavelength of the lowest-mass pion.

This paper is organized as follows. We will give the numerical details of the calculation in Sec. 2. In Sec. 3, we shall discuss the effect of the zero modes in the meson propagators. In view of the fact that the scalar condensate contains a term from the zero modes (which goes away at the infinite volume), through the generalized Gell-Mann-Oakes-Renner (GOR) relation, the pseudoscalar correlator should also be contaminated by the zero mode contribution. We have observed the effect of the zero modes in the pseudoscalar propagator at small quark mass. After clarifying the zero mode issue, we proceed to calculate the non-perturbatively determined renormalization constant Z_A from the axial Ward identity and the pion decay constant f_π . We find that f_π is free of the quenched chiral log singularity, is very independent of the quark mass, and is thus a good quantity to set the lattice scale. We present the results in Sec. 4. In Section 5, we explain our effort in searching for the predicted quenched chiral logs. We don't see the chiral logs in the pseudoscalar masses and the ratio of pseudoscalar masses with unequal quark masses to those with equal masses. We only see it in the pseudoscalar matrix element f_P and the f_P/f_π ratio at very small quark masses. Presumably it is relatively easy to see in f_P/f_π due to its divergent nature with respect the the quark mass. A summary is given in Sec. 6.

2 Numerical Details

For Neuberger's overlap fermion [2], we adopt the following form for the massive Dirac operator [11, 12, 8]

$$D(m_0) = (1 - \frac{m_0 a}{2\rho})\rho D(\rho) + m_0 a, \quad (1)$$

where

$$D(\rho) = 1 + \gamma_5 \epsilon(H), \quad (2)$$

so that

$$D(m_0) = \rho + \frac{m_0 a}{2} + (\rho - \frac{m_0 a}{2})\gamma_5 \epsilon(H), \quad (3)$$

where $\epsilon(H) = H/\sqrt{H^2}$ is the matrix sign function and H is taken to be the hermitian Wilson-Dirac operator, i.e. $H = \gamma_5 D_w$. Here D_w is the usual Wilson fermion operator, except with a negative mass parameter $-\rho = 1/2\kappa - 4$ in which $\kappa_c < \kappa < 0.25$. We take $\kappa = 0.19$ in our calculation which corresponds to $\rho = 1.368$. The massive overlap action is so defined so that the tree-level renormalization of mass and wavefunction is unity. The bare mass parameter m_0 * is proportional to the quark mass without an additive constant which we have verified numerically in a previous study [7].

We adopt the optimal rational approximation [13, 7] to approximate the matrix sign function. The inversion of the quark matrix involves nested do loops in this approximation. It is found that it is cost effective to project out a relatively few eigenmodes with very small eigenvalues in the operator H^2 in order to reduce the condition number and speed up the convergence in the inner do loop [4, 7]. At the same time, it improves chiral symmetry relations such as the Gell-Mann-Oakes-Renner relation [7]. However, it is shown [14] that the density of these small eigenmodes grows as $e^{\sqrt{a}}$ with a being the lattice spacing. As a result, it is very costly and impractical to work on large volumes with the lattice spacings currently used. There are simply too many small eigenmodes to be projected out.

For this reason, we explore other options to clear this hurdle. We have tested the tree-level tadpole-improved Lüscher-Weisz gauge action [15] and find that the density of these small eigenvalue modes is decreased to a point that it becomes feasible to go to large volumes with a size of the lattice 3 times of the Compton wavelength of the lightest pion. We further find that the anisotropic action [17] requires projection of more small eigenvalues in H^2 in order to achieve the same convergence in the inner loop than does the isotropic one. Thus, we decide to use the isotropic action. We also find that using the clover action with either sign requires the projection of more small eigenvalue modes. Therefore we use the Wilson action for H in the Neuberger operator with $\kappa = 0.19$. On a 20^4 lattice with $\beta = 7.60$ tree-level tadpole-improved Lüscher-Weisz gauge action, we project out 80 small eigenvalues. Beyond these eigenmodes,

*Note that we used a different action before in [7]. As a result the bare mass here is equal to ρ times the bare mass in [7].

the level density becomes dense. As a result, the number of conjugate gradient steps is about 345 for the inner loop and about 300 for the outer loop. These numbers are about a factor of 2 larger than those for the Wilson gauge action on small volumes [7]. Therefore, other than the overhead of projecting out the small eigenvalue modes, the cost scales linearly with volume.

Since the conjugate gradient algorithm accommodates multiple masses with a minimum overhead, we calculated 16 quark masses with $m_0a = 0.01505, 0.01642, 0.01915, 0.02736, 0.04104, 0.05472, 0.06840, 0.08208, 0.09576, 0.1094, 0.1368, 0.1642, 0.1915, 0.2189, 0.2462, 0.2736$. For the masses $m_0a = 0.01505, 0.01642, 0.06840, 0.09576, 0.1368, 0.1915, 0.2462$, we have only 25 configurations. $m_0a = 0.04104$ has 53 configurations. The rest all have 63 gauge configurations. From the string tension with $\sqrt{\sigma} = 440$ MeV, we find that $a = 0.13$ fm. However, as we shall see later in Section 4, the scale determined from f_π is 0.157 fm which makes the physical length of the lattice to be 3.14 fm. The smallest pion mass turns out to be ~ 200 MeV so that the size of the lattice is ~ 3 times of the Compton wavelength of the lowest mass pion and more than 3 times for the heavier ones.

We adopt the periodic boundary condition for the spatial dimensions and the fixed boundary condition in the time direction so that we can have effectively a longer range of time separation between the source and sink to examine the meson propagators with small quark masses which lead to longer correlation lengths. The source of the meson interpolation field is placed at the 3rd time slice and we consider the sink as far as the 17th time slice to mitigate the boundary effect. This gives us a time separation of 14.

We have varied statistics for different quark masses. Of the 16 cases, 7 have 25 gauge configurations, one has 53, and the remaining 8 have 63 configurations. In order to carry out correlated fits to extrapolate observables to the physical pion mass, we construct the covariance matrix by embedding the one with smaller dimension, e.g. 25 and 53 into the one with dimension 63 in a block diagonal form. For example, the covariance C_{ij} for the one with 25 configurations is constructed so that $C_{ij}(i \leq 25, j > 25) = 0, C(i > 25, j \leq 25) = 0$ and $C_{ij}(i, j > 25) = \delta_{ij}$.

3 Zero Mode Effects in Meson Propagators

The quark zero mode is known to contribute to the vacuum scalar density $\langle \bar{\psi}\psi \rangle$ on a finite volume. The latter can be written in the following form for small quark mass m_0 [†]

[†]We shall address the quenched chiral log issue separately in Sec. 5.

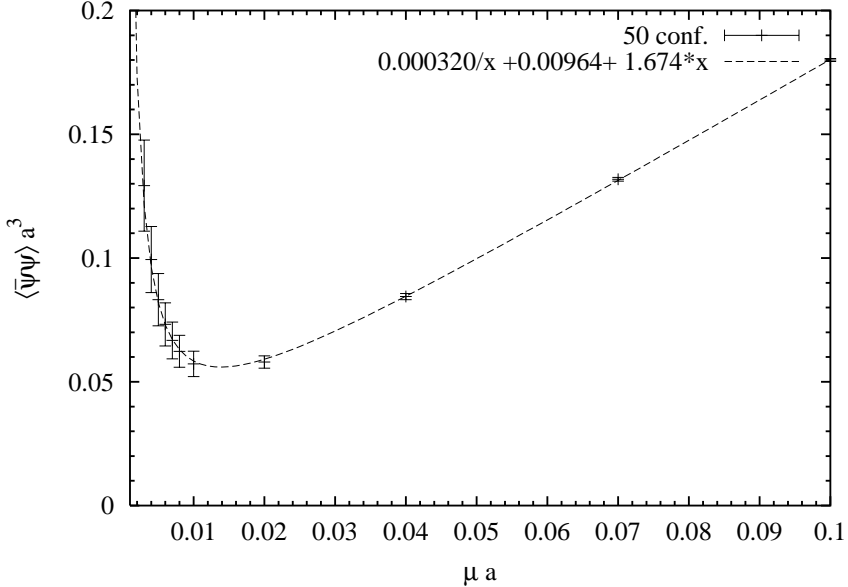


Figure 1: $\langle\bar{\psi}\psi\rangle$ as a function of the quark mass. We used 50 configurations of a $6^3 \times 12$ lattice with Wilson gauge action at $\beta = 5.7$. Here $\mu a = m_0 a / 2\rho$.

$$-\langle\bar{\psi}\psi\rangle = \frac{\langle|Q|\rangle}{m_0 V} + c_0 + c_1 m_0, \quad (4)$$

where Q is the topological charge which, according to the Atiya-Singer theorem, is the difference between the number of left-handed and right-handed zero modes (i.e. $Q = n_- - n_+$) and has been shown to hold for overlap fermions or other local fermion actions which satisfy the Ginsparg-Wilson relation [18, 19]. Since $\langle|Q|\rangle$ grows as \sqrt{V} , the zero mode contribution goes away at the infinite volume limit while keeping m_0 fixed at a non-zero value. Thus the quark condensate which is the infinite volume and zero mass limit of $\langle\bar{\psi}\psi\rangle$ is represented by c_0 in Eq. (4). However, on a fixed finite volume lattice, this zero mode contribution is divergent for small enough m_0 . This was first observed in the domain-wall formulation [20] and is also seen in the overlap fermion [21]. Here we reproduce it in Fig. 1 which shows the divergent part of $\langle\bar{\psi}\psi\rangle$ from the zero modes for a $6^3 \times 12$ lattice with the Wilson gauge action at $\beta = 5.7$.

We see from Fig. 1 that c_0 is non-zero in this range of the quark mass and upon extrapolation to the infinite volume first before taking the chiral limit is the definition of the quark condensate $-\Sigma$. However, if one keeps volume fixed and lets the quark mass approach zero, e.g. $m_0 a < 0.001$, it is then found [4, 5, 21] that c_0 becomes zero. It is known [22] that when the size of the lattice is much smaller than the pion Compton wavelength, i.e. $L \ll 1/m_\pi$, the constant term vanishes and $\langle\bar{\psi}\psi\rangle$ is proportional to $m_0 \Sigma^2 V$ for small masses aside from the $\frac{\langle|Q|\rangle}{m_0 V}$ term. Using finite size scaling, the chiral condensate Σ can be extracted [5].

While we have a reasonably good understanding of the role of zero modes in $\langle\bar{\psi}\psi\rangle$, their role in the hadron propagators is only beginning to be investigated in

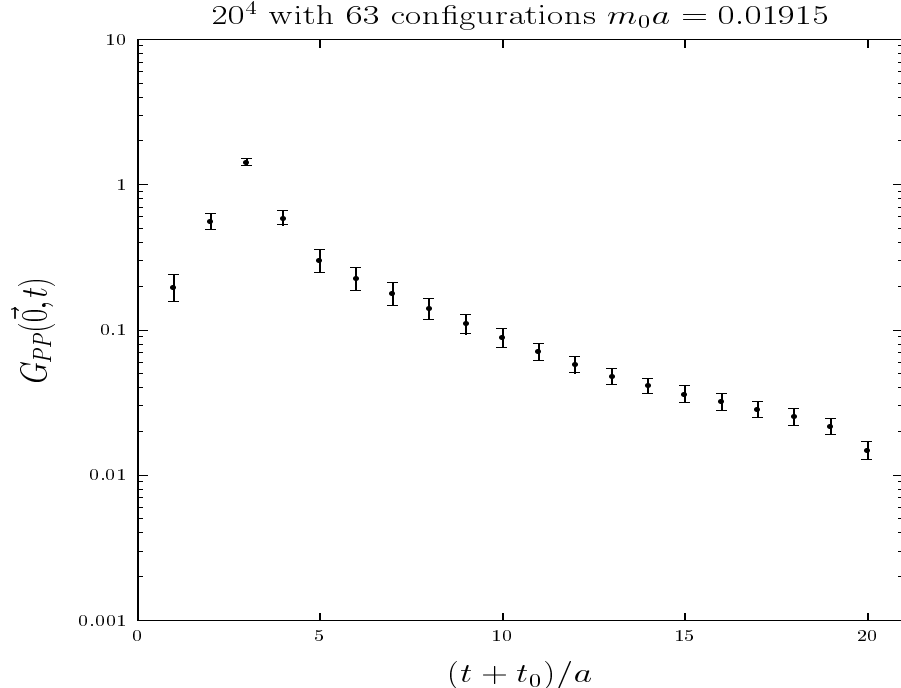


Figure 2: Pion propagator for $m_0a = 0.01914$ for all 63 configurations. The source is placed at $t_0/a = 3$

the domain-wall formalism [23] and its detailed influence on the hadron propagators is not fully understood. We shall investigate it in the pseudoscalar meson channel. There has been some concern about the behavior of the pion mass. It is not clear if it approaches zero in a finite volume in the chiral limit. In fact, one finds that the pion mass squared appears to approach a non-zero value on small lattices [24, 25]. To understand the situation, we first examine the generalized Gell-Mann-Oakes-Renner (GOR) relation

$$\frac{2(2m_0)^2}{V} \int d^4x d^4y \langle \pi^a(x) \pi^a(y) \rangle = -2m_0 \langle \bar{\psi} \psi \rangle. \quad (5)$$

The left hand side of Eq. (5) also has a contribution of $\frac{2\langle |Q| \rangle}{V}$ as does on the right hand side. Assuming the remainder of the pseudoscalar susceptibility is dominated by the pion, it is approximately $-f_\pi^2 m_\pi^2$. Comparing with Eq. (4), we get

$$f_\pi^2 m_\pi^2 = 2m_0 c_0 + 2m_0^2 c_1. \quad (6)$$

From this we see that m_π^2 approaches zero as m_0 for those volumes where c_0 is non-zero. On the other hand, when the m_0 is so small that c_0 becomes zero for certain fixed volume, the r.h.s. of Eq. (6) is survived by the next leading term with c_1 which is proportional to m_0^2 . As a result, one expects that m_π to be linearly proportional to m_0 . Here we have ignored the complication due to the quenched chiral log which we will address in Section 5.

Next, we turn to the zero-momentum pseudoscalar propagator $\int d^3x \langle \pi^a(x) \pi^a(0) \rangle$

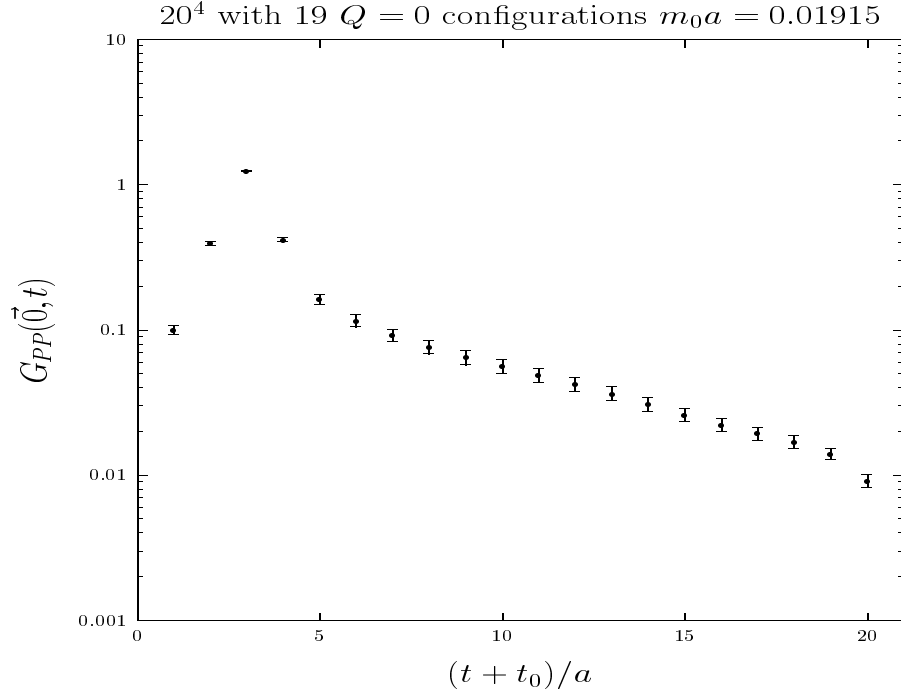


Figure 3: Pion propagator for $m_0a = 0.01914$ for 19 configurations with $Q = 0$.

which has two terms due to the zero modes as pointed out in the study of domain wall fermions [23]

$$\begin{aligned} \int d^3x \langle \pi(x) \pi(0) \rangle &= \int d^3x \left[\sum_{i,j=\text{zero modes}} \frac{tr(\psi_j^\dagger(x) \psi_i(x)) tr(\psi_i^\dagger(0) \psi_j(0))}{m_0^2} \right. \\ &\quad \left. + 2 \sum_{i=0, \lambda > 0} \frac{tr(\psi_\lambda^\dagger(x) \psi_i(x)) tr(\psi_i^\dagger(0) \psi_\lambda(0))}{m_0(\lambda^2 + m_0^2)} + \frac{|\langle 0 | \pi(0) | \pi \rangle|^2 e^{-m_\pi t}}{2m_\pi} \right] \end{aligned} \quad (7)$$

The first term is purely the zero-mode contribution. The second term is the cross term between the zero modes and the non-zero modes. We have used the property that the non-zero modes come in pairs which are related by γ_5 , i.e. $\gamma_5 \psi_\lambda = \psi_{-\lambda}$. Upon integrating the propagator with respect to time, we find

$$\int d^4x \langle \pi(x) \pi(0) \rangle = \frac{\sum_{i=0} tr(\psi_i^\dagger(0) \psi_i(0))}{m_0^2} + \frac{\sum_{i=0, \lambda > 0} \delta_{i\lambda} tr(\psi_i^\dagger(0) \psi_\lambda(0))}{m_0(\lambda^2 + m_0^2)} + \frac{|\langle 0 | \pi(0) | \pi \rangle|^2}{2m_\pi^2}. \quad (8)$$

Comparing with the generalized GOR relation in Eq. (5), we see the first term corresponds to $\frac{\langle |Q| \rangle}{m_0 V}$ term in Eq. (4) and the second term vanishes due to the orthogonality between the zero modes and the non-zero modes. In either case, we expect that the number of zero modes grows with \sqrt{V} and the eigenfunction $\psi(0) \propto 1/\sqrt{V}$. As a result, both zero-mode terms in Eqs. (7) and (8) goes down with volume like $1/\sqrt{V}$ and are finite volume artifacts.

The most straight-forward way of isolating the zero mode contribution is to calculate their eigenvectors and project them out. However, this is very costly, as costly as calculating the quark propagator itself.

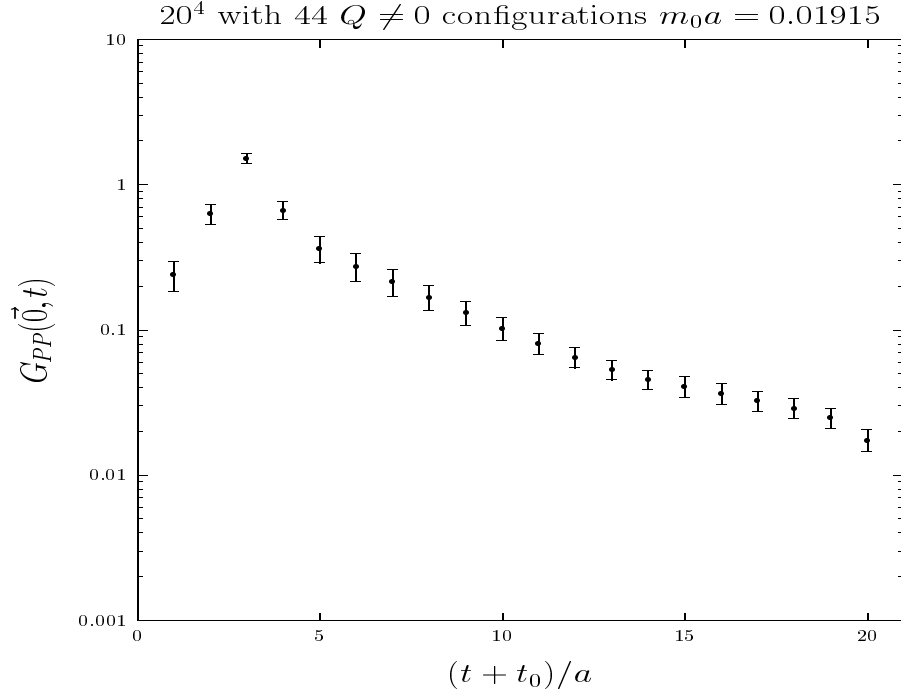


Figure 4: The same as in Fig. 3 for 44 configurations with $Q \neq 0$.

We show the pseudoscalar propagator for a light quark mass ($m_0a = 0.01915$) in Fig. 2 and we see that their appears a kink at $t/a \sim 8 - 9$ (The source is placed at $t_0/a = 3$ so that it appears at $(t + t_0)/a \sim 11 - 12$). To further explore its origin, we separate the 63 configurations into 19 with trivial topology (i.e. $Q = 0$) and 44 with non-trivial topology (i.e. $Q \neq 0$) and plot the respective pseudoscalar propagators in Figs. 3 and 4.

We see that the propagator on the $Q = 0$ configurations (Fig. 3) has a single exponential all the way from $t/a = 5$ to 14. Upon fitting a single exponential in this range, we find $m_Pa = 0.153(12)$. On the other hand, the propagator of the $Q \neq 0$ configurations (Fig. 4) still has a pronounced kink at $t/a \sim 8$. When we fit it in the range $t/a = 8 - 14$, the mass is $m_Pa = 0.146(32)$ which is quite consistent with that from the $Q = 0$ configurations. On the other hand, when we fit the time range from 4 to 8, $m_Pa = 0.245(58)$ which is quite a bit higher than that of the $Q = 0$ configurations. We take this as the evidence that the zero-mode contributions, the combined direct and cross terms, falls off faster in t/a than the pseudoscalar mass. We can thus use the time separation as the filter to obtain the masses and decay constants of the physical pseudoscalar mesons. Now we can understand why in the previous studies of m_P , the m_P^2 does not approach zero with the quark mass [24, 25]. In Ref. [24], the lattice size is $6^3 \times 12$ with $\beta = 5.7$. Since it is using the fixed boundary condition in the time direction, the maximum usable time separation is about 7. This translates into time separation of ~ 9 on our lattice. In Ref. [25], the lattice size is

$12^3 \times 24$ with $\beta = 5.9$. In this study, the authors use the periodic boundary condition in time, time slices up to 12 are fitted which corresponds to ~ 10 on our lattice. In either case, the fitted time range is expected to be contaminated by the zero mode contribution and result in a higher mass for a given quark mass. To verify this, we fit our data in the time range $t/a = 5 - 9$ and plot the resulting $m_P^2 a^2$ in Fig. 5. We see that they indeed don't approach zero with a fit linear and quadratic in $m_0 a$ (dashed line), similar to those shown in Refs. [24, 25]. One may attempt to interpret the data to include a chiral log and force the pion mass to go to zero at the chiral limit. This can be misleading. We shall defer the discussion of the complication due to the quenched chiral log in Section 5.

In contrast, we plot in Fig. 6 $m_P^2 a^2$ from the longer range of t/a , i.e. after $t/a = 7$ and see that they are lower and do approach zero with $m_0 a$. We fit them with both a linear mass dependence from the smallest mass up to $m_0 a = 0.1094$ (10 points) and a linear plus quadratic fit up to $m_0 a = 0.1642$ (12 points). The results are

$$\begin{aligned} m_P^2 a^2 &= -0.00005(288) + 1.63(4)m_0 a, \quad \chi^2/DF = 0.2, \\ m_P^2 a^2 &= 0.0008 + 1.60(11)m_0 a + 0.20(63)m_0^2 a^2, \quad \chi^2/DF = 0.25 \end{aligned} \quad (9)$$

We find that the intercept is consistent with zero which confirms the prediction of the generalized GOR relation that m_P does approach zero in a fixed volume as long as one avoids the finite volume artifacts due to the zero modes.

The zero mode contribution to mesons can be written as

$$\int d^3x \langle M(x)M(0) \rangle|_{\text{zeromodes}} = \quad (10)$$

$$\begin{aligned} & - \int d^3x \left[\sum_{i,j=\text{zeromodes}} \frac{\text{tr}(\psi_j^\dagger(x)\gamma_5\Gamma\psi_i(x))\text{tr}(\psi_i^\dagger(0)\bar{\Gamma}\gamma_5\psi_j(0))}{m_0^2} \right. \\ & \left. + 2 \sum_{i=0,\lambda>0} \frac{\text{tr}(\psi_\lambda^\dagger(x)\gamma_5\Gamma\psi_i(x))\text{tr}(\psi_i^\dagger(0)\bar{\Gamma}\gamma_5\psi_\lambda(0))}{m_0(\lambda^2 + m_0^2)} \right], \end{aligned} \quad (11)$$

where Γ and $\bar{\Gamma}$ are the gamma matrices for the corresponding meson interpolation fields. For the pseudoscalar meson as we discussed above, $\Gamma = -\bar{\Gamma} = \gamma_5$. For the scalar meson (the connected insertion part), $\Gamma = \bar{\Gamma} = 1$. Since the zero modes are the eigenstates of γ_5 , i.e. $\gamma_5\psi_{i=0} = \pm\psi_{i=0}$, the zero mode contribution in the scalar propagator has a negative sign from that in the pseudoscalar propagator. Thus, it is suggested [23, 6] to consider $\int d^3x [\langle \pi(x)\pi(0) \rangle + \langle \sigma(x)\sigma(0) \rangle]$ where the zero-mode contributions cancel and at large t/a it should be dominated by the pseudoscalar. However, there is a problem.

As will be shown in a separate publication [26], the large time part of the isovector-scalar propagator for the quark mass range that we are concerned turns out to be negative. It is pointed out in a study with pole-shifting in the Wilson action [27] that it is dominated by the would-be η' and π intermediate state which is negative due

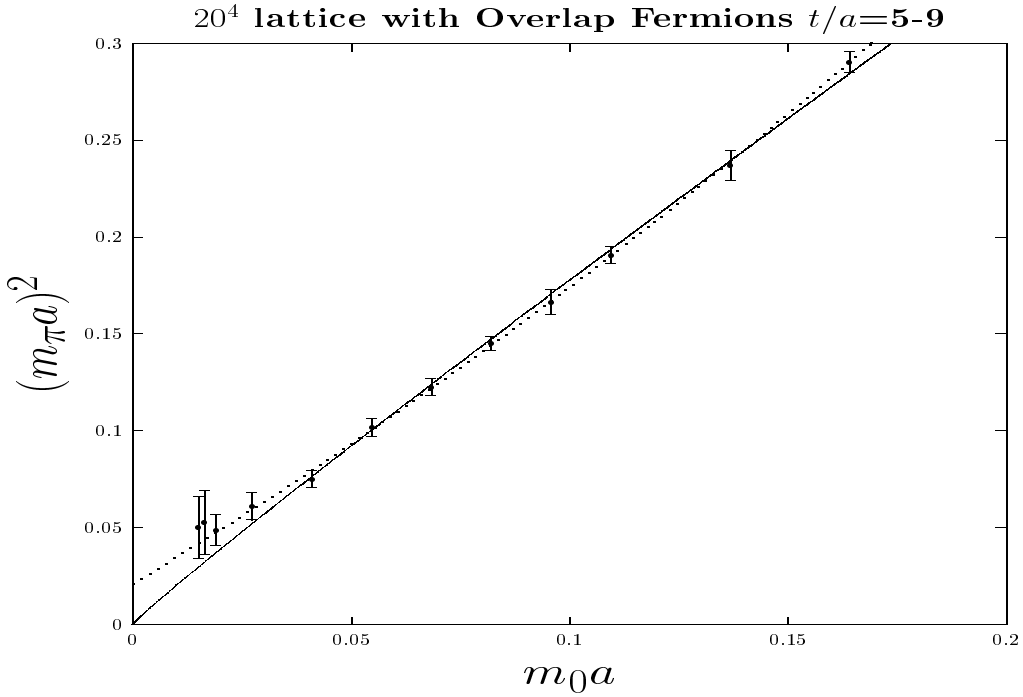


Figure 5: $m_P^2 a^2$ vs $m_0 a$ with a fit of $m_P a$ in the window of $t/a = 5 - 9$. The dashed line is a fit linear and quadratic in $m_0 a$. The solid line is a fit including the chiral log.

to quenching. In the intermediate time region, there is still the contribution from η' and π intermediate state besides the a_0 . As a consequence, the addition of the pseudoscalar and scalar meson is not a viable solution to obtaining the pseudoscalar mass. It is also suggested that the axial-vector interpolation field with $\Gamma = \bar{\Gamma} = \gamma_4 \gamma_5$ does not have the direct term contribution from the zero modes since all the zero modes have the same chirality in a given gauge configuration. However, the second term in Eq. (10) may still have a contribution. Since it is a cross term, it might be small due to cancellations. Unfortunately, our data on the $\langle A_4 A_4 \rangle$ correlator are much noisier than the $\langle \pi \pi \rangle$ correlator, since $\langle 0 | A_4 | \pi(0) \rangle = \sqrt{2} m_\pi f_\pi$ which diminishes when the pion mass is small. We cannot conclude anything from them.

It appears that, short of projecting out the zero modes from the meson propagators, fitting the mass in the time range longer than that being contaminated by the zero modes from the $\langle \pi \pi \rangle$ correlator is probably the only practical way of getting reliable and accurate pseudoscalar masses.

4 Z_A and Pion Decay Constant f_π

It has been pointed out in our earlier work [7] that the renormalization constant Z_A for the axial current $A_\mu = \bar{\psi} (i \gamma_\mu \gamma_5 (1 - D/2)) \psi$ can be obtained through the axial

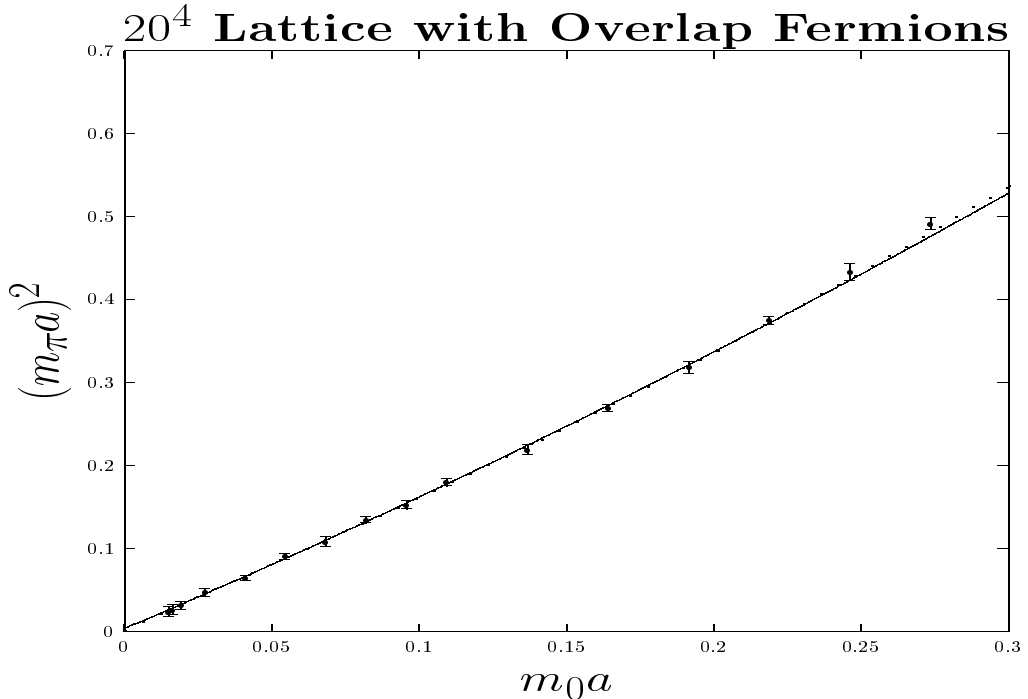


Figure 6: $m_P^2 a^2$ vs $m_0 a$ with t/a in between 7 and 16 depending on the quark mass. The linear plus quadratic fit (solid line) and the chiral log fit (dashed line) to be discussed later for the smallest 14 quark masses are drawn.

Ward identity

$$Z_A \partial_\mu A_\mu = 2Z_m m_0 Z_P P, \quad (12)$$

where $P = \bar{\psi}(i\gamma_5(1-D/2)\psi)$ is the pseudoscalar density. Since $Z_m = Z_S^{-1}$ and $Z_S = Z_P$ due to the fact the scalar density $\bar{\psi}(1-D/2)\psi$ and the pseudoscalar density P are in the same chiral multiplet, Z_m and Z_P cancel in Eq. (12) and one can determine Z_A non-perturbatively from the axial Ward identity using the bare mass m_0 and bare operator P . To obtain Z_A , we shall consider the on-shell matrix elements between the vacuum and the zero-momentum pion state for the axial Ward identity

$$Z_A \langle 0 | \partial_\mu A_\mu | \pi(\vec{p} = 0) \rangle = 2m_0 \langle 0 | P | \pi(\vec{p} = 0) \rangle, \quad (13)$$

where the matrix elements can be obtained from the zero-momentum correlators

$$\begin{aligned} G_{\partial_4 A_4 P}(\vec{p} = 0, t) &= \langle \sum_{\vec{x}} \partial_4 A_4(x) P(0) \rangle \\ G_{PP}(\vec{p} = 0, t) &= \langle \sum_{\vec{x}} P(x) P(0) \rangle. \end{aligned} \quad (14)$$

The non-perturbative Z_A is then

$$Z_A = \lim_{t \rightarrow \infty} \frac{2m_0 G_{PP}(\vec{p} = 0, t)}{G_{\partial_4 A_4 P}(\vec{p} = 0, t)}. \quad (15)$$

Z_A thus calculated for all the quark masses are plotted in Fig. 7.

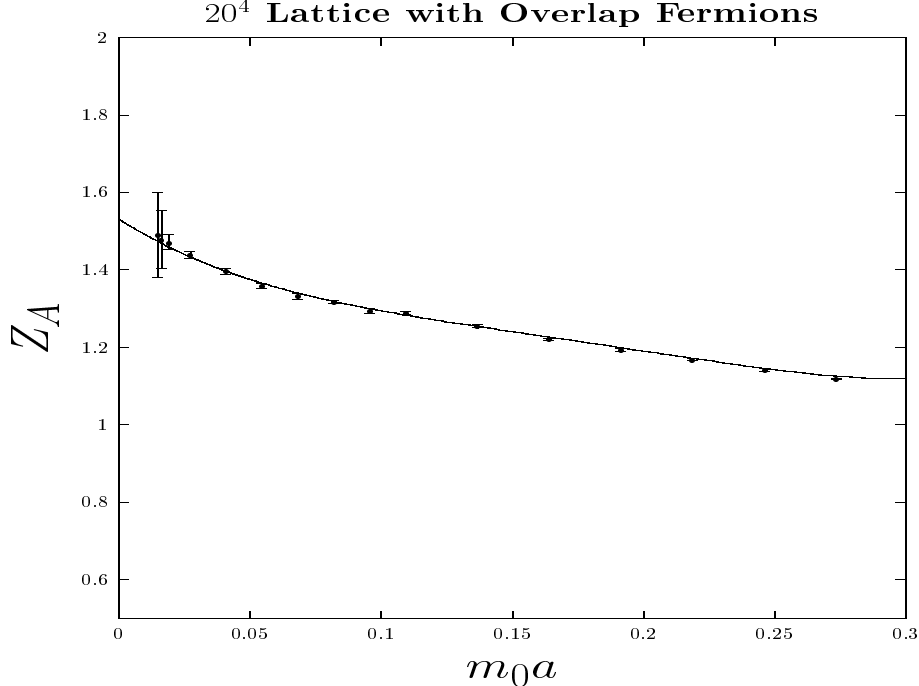


Figure 7: Z_A vs quark mass m_0a . The solid line is the fit from Eq. (16)

Save for the last two points at the smallest masses ($m_0a = 0.01505$ and 0.01642), the errors are small. We have fitted them as a function of the quark mass. A power-series fit for all the 16 points with m_0a from 0.01505 to 0.2736 gives

$$Z_A = 1.531(17) - 4.28(60)m_0a + 28.4(69)(m_0a)^2 - 108(32)(m_0a)^3 + 152(50)(m_0a)^4, \quad (16)$$

with $\chi^2/DF = 0.4$. We see that at the chiral limit, Z_A is determined to about 1% precision. We find it to be larger than the perturbative calculation [11] which gives $Z_A(\mu = 1/a) = 1.213$ for Wilson gauge action with $\beta = 5.85$ which has about the same string tension as our gauge configurations.

For the pion decay constant, one can look at the ratio of the zero-momentum correlator

$$G_{A_4 P}(\vec{p} = 0, t) = \langle \sum_{\vec{x}} A_4(x) P(0) \rangle, \quad (17)$$

and $G_{PP}(\vec{p} = 0, t)$,

$$f_\pi a = \lim_{t \rightarrow \infty} \frac{Z_A G_{A_4 P}(\vec{p} = 0, t)}{\sqrt{m_\pi a G_{PP}(\vec{p} = 0, t)}} e^{m_\pi t/2}. \quad (18)$$

Combining with Z_A from Eq. (15), we obtain

$$f_\pi a = \lim_{t \rightarrow \infty} \frac{2m_0a \sqrt{G_{PP}(\vec{p} = 0, t)} G_{A_4 P}(\vec{p} = 0, t)}{\sqrt{m_\pi a} G_{\partial_t A_4 P}(\vec{p} = 0, t)} e^{m_\pi t/2}. \quad (19)$$

We first fit the pion masses from $G_{PP}(\vec{p} = 0, t)$ and feed them into Eq. (19). The errors of the ratio are obtained with the jackknife method. We plot the result in Fig. 8 as a function of m_0a .

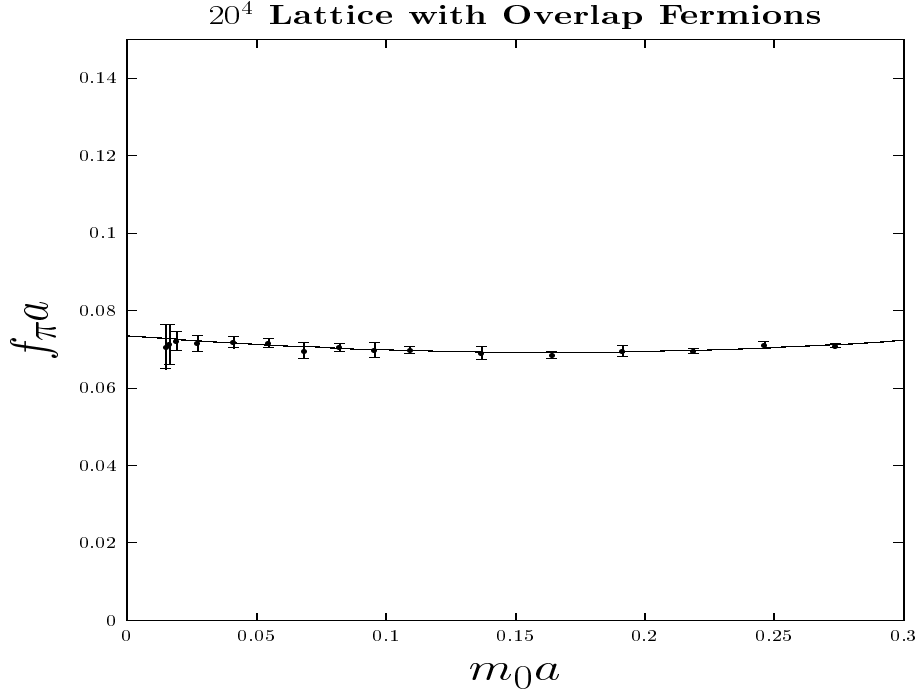


Figure 8: Renormalized $f_\pi a$ vs quark mass $m_0 a$.

We see that it is fairly constant in the quark mass range that we have calculated. With all 16 data points in a linear plus quadratic fit, we find

$$f_\pi a = 0.0735(12) - 0.053(17)m_0 a + 0.16(5)(m_0 a)^2, \quad (20)$$

with $\chi^2/DF = 0.18$. Due to its constancy, it yields an error of only 1.6% in the chiral limit. Given that it is a physical observable from the fermion operator without the chiral log in a quenched theory [28] and with such high precision, it is an ideal quantity to set the scale of the lattice. Comparing with the experimental value $f_\pi = 92.4$ MeV, we determine the scale of our lattice to be $a = 0.157(3)$ fm. This is about 22% higher than that determined from the string tension with $\sqrt{\sigma} = 440$ MeV and 27% larger than that determined from r_0 . This is quite consistent with other quenched calculations.

5 Quenched Chiral Logs

In the quenched approximation of QCD, one ignores the virtual quark loops. One of the consequences is that the flavor-singlet meson propagator (which we shall refer to as η' even though the physical η' is not completely flavor-singlet and has octet mixture) has a double pole in the Veneziano model for the U(1) anomaly [29, 30]. As such, it does not move the mass of the would-be Goldstone boson to the large η'

mass. Consequently, this leads to infrared singular η' loops with the hair-pin type diagrams in the renormalization of hadron masses and certain matrix elements and thus alters their chiral behaviors from those of full QCD with dynamical fermions.

The first study of the anomalous chiral behavior was done by Sharpe [28] and Bernard and Golterman [31] in quenched chiral perturbation theory. They predicted the chiral-log pathologies in the pseudoscalar meson masses, $\langle\bar{\psi}\psi\rangle$, the f_K/f_π ratio, etc. The first evidence of the chiral-log was observed by the CPPACS Collaboration [32] in the ratio of pseudoscalar meson masses with two unequal quark masses with the Wilson fermion. They obtain the chiral log parameter $\delta = 0.8 - 1.2$. A more extensive study [33] which invokes the shifting of the real poles of the quark propagator to improve the otherwise poor chiral property of the Wilson fermion near the chiral limit was carried out to examine the quenched chiral logs in the pseudoscalar masses and the pseudoscalar decay constants and obtain consistent results with $\delta = 0.065 \pm 0.013$. Both of them are small compared to that expected from the coupling of the would-be Goldstone bosons (or quark loops in the pseudoscalar channel) which is responsible for the η' mass of the U(1) anomaly. Recently, the small nonzero eigenvalues of the Overlap Dirac operator were calculated in a deconfined phase [34] and it was found that the chiral condensate diverges at the infinite volume limit indicating a quenched singularity consistent with the quenched chiral perturbation prediction $\langle\bar{\psi}\psi\rangle \propto m^{\frac{-\delta}{1+\delta}}$.

Given that the overlap fermion has the promise of exact chiral symmetry on the lattice, it is natural to look for these chiral singularities and check if the quenched chiral logs seen in the Wilson fermion can be verified with the overlap action. The first attempt to extract the chiral log from the pion mass on several small volumes was inconclusive [7]. We shall examine them here on a much larger volume.

The behavior of the quenched chiral logs can be seen from the sigma model [33] with $U(3) \times U(3)$ where the pseudoscalar field is represented by

$$U = e^{\phi_0/f} e^{i \sum_{a=1}^8 \lambda_a \phi_a/f}, \quad (21)$$

where λ_a is the SU(3) flavor matrix and ϕ_a are the octet Goldstone boson fields. The U(1) part is described by η' field with $\phi_0 = \sqrt{2/N_f} \eta'/f$ where N_f is the number of flavor which is 3 in our case. The effect of the chiral logs can be understood as the renormalization effect by integrating out the η' [33]. The resulting $SU(3) \times SU(3)$ will be represented by the renormalized U

$$U = e^{-\langle\phi_0^2\rangle/2f^2} e^{\sum_{a=1}^8 \lambda_a \phi_a/f}. \quad (22)$$

In the quenched approximation, the integral representing the η' loop involves only the hair-pin diagram of two would-be singlet Goldstone boson (we shall refer it as η and has the same mass as π) propagators

$$\langle\phi_0^2\rangle = \frac{2}{VN_f} \int d^4x \langle\eta(x)\eta(x)\rangle = \int \frac{d^4p}{(2\pi)^4 N_f} \frac{-\bar{m}_0^2}{p^2 + m_\pi^2} = \frac{-\bar{m}_0^2}{16\pi^2 N_f} \left(\ln \frac{\lambda^2}{m_\pi^2} - 1\right) \quad (23)$$

Therefore, the infrared singular part of U in Eq. (22) can be represented by δ

$$U = e^{-\delta \ln m_\pi^2} e^{\sum_{a=1}^8 \lambda_a \phi_a / f} = \left(\frac{1}{m_\pi^2}\right)^\delta e^{\sum_{a=1}^8 \lambda_a \phi_a / f}, \quad (24)$$

where

$$\delta = \frac{\bar{m}_0^2}{16\pi^2 N_f f^2}. \quad (25)$$

From the Witten-Veneziano model of the η' mass, $\bar{m}_0 \sim 870$ MeV. This gives an estimate of $\delta = 0.183$.

To see the effects on various physical quantities, one can first look at pseudoscalar density and axial current operator [33]. In the sigma model,

$$\begin{aligned} \bar{\psi} i \gamma_5 \psi &\propto U - U^\dagger \\ \bar{\psi} i \gamma_\mu \gamma_5 \psi &\propto i[U^{-1} \partial_\mu U - (\partial_\mu U^{-1})U]. \end{aligned} \quad (26)$$

With U given in Eq. (24), one arrives at

$$\begin{aligned} f_P &= \langle 0 | \bar{\psi} i \gamma_5 \psi | \pi(\vec{p} = 0) \rangle = \left(\frac{1}{m_\pi^2}\right)^\delta \tilde{f}_P \\ f_\pi &= \langle 0 | \bar{\psi} i \gamma_\mu \gamma_5 \psi | \pi(\vec{p} = 0) \rangle / \sqrt{2} m_\pi = \tilde{f}_\pi \end{aligned} \quad (27)$$

where f_P is the pseudoscalar decay constant and f_π is the axial decay constant and \tilde{f}_P and \tilde{f}_π are constants for small quark masses. Thus, one expects that f_P is singular as the quark masses approaches zero in the quenched approximation; whereas f_π remains a constant. From the axial Ward identity in Eq. (12) and Eq. (27), one expects

$$m_\pi^2 \propto m_q \frac{f_P}{f_\pi} \propto m_q \left(\frac{1}{m_\pi^2}\right)^\delta, \quad (28)$$

where m_q is the quark mass and therefore

$$m_\pi^2 \propto m_q^{\frac{1}{1+\delta}} \quad (29)$$

which is the behavior predicted in quenched χPT [28].

We first fit the form in Eq. (29) for a range of small quark mass points (6 to 10). We find that δ ranges from 0.000(40) to 0.020(71) with a $\chi^2/DF \sim 0.23$. Since the errors are much larger than the central values and the χ^2/DF is not much better than the linear and the linear plus quadratic fits in Eq. (9), we conclude that one does not see the chiral log in m_π^2 . We have also fitted them with the form [31, 32]

$$m_\pi^2 = 2A m_0 \{1 - \delta[\ln(2A m_0 / \Lambda_\chi^2) + 1]\} + 4B m_0^2 + C, \quad (30)$$

where we add a constant C to consider the possible intercept at the chiral limit. The best fit which gives constant values of A , B , and C for a range of $\Lambda_\chi = 0.6$ GeV to

1.4 GeV are with the last 10 points from the smallest quark mass to $m_0a = 0.1094$ where $m_Pa = 0.424(5)$. It turns out that $C = -0.005(27)$ consistently. A and B are also stable. δ ranges from 0.16(75) to 0.24(185) with $\chi^2/DF = 0.28$. Again, we find that the errors of δ are much larger than their respective central values. Again, there is no evidence for δ in m_π^2 . We plot the fit with the log form for the last 14 points in Fig. (2) as the dashed line in Fig. 6. We see that one cannot distinguish it from the linear plus quadratic fit (solid line) in the range of fit involving 14 smallest quark masses. Since it is hard to see δ in the form of $m_q^{\frac{1}{1+\delta}}$, we examined instead

$$m_\pi^2/m_q \propto m_q^{\frac{-\delta}{1+\delta}} \quad (31)$$

in the hope of seeing the singularity. Unfortunately, the errors are so large that one cannot conclude anything from this expression.

We should point out that if we use the $m_P^2a^2$ data from the shorter time range such as the one with $t/a = 5 - 9$ as plotted in Fig. 5 and insist on fitting them with a power form in Eq. (29), we find that one can find a fit with the last 12 mass points that $\delta = 0.054 \pm 0.028$ with $\chi^2/DF = 0.98$. This is plotted as the solid line in Fig. 5. This serves as a caveat to show that one can misconstrue the contamination of the zero modes as the chiral log.

Next we examine the pseudoscalar meson mass ratios. The quenched χPT calculation [31] suggests the following form for the squared mass of a pseudoscalar meson made with quark and antiquark masses m_i and m_j

$$m_{Pij}^2 = A(m_i + m_j) \{1 - \delta[\ln(2Am_i/\Lambda_\chi^2) + m_j/(m_j - m_i) \ln(m_j/m_i)]\} + B(m_i + m_j)^2 + C. \quad (32)$$

When δ is small and B is negligible, then one can form a mass ratio whose deviation from unity is directly proportional to δ [32, 33]

$$y_{ij} = \frac{2m_i}{m_i + m_j} \frac{m_{Pij}^2}{m_{Pii}^2} \frac{2m_j}{m_i + m_j} \frac{m_{Pij}^2}{m_{Pjj}^2} = 1 + \delta x_{ij}, \quad (33)$$

where

$$x_{ij} = 2 + \frac{m_i + m_j}{m_i - m_j} \ln(m_j/m_i). \quad (34)$$

Since this ratio is valid when the quadratic mass term B is negligible, we shall restrict our data to those quark masses where the m_{Pii}^2 is mostly linear in m_i . As we can see from Fig. 6, this means that we should be considering quark mass $m_0a \leq 0.1094$. Above that, $m_P^2a^2$ curves upward which will require a B term. We take the lowest 5 quark masses with the same 63 configurations, i.e. $m_0a = 0.01915, 0.02736, 0.05472, 0.08208$, and 0.1094 to form the ratio in Eq. (33). With a linear fit in x_{ij} in Eq. (33), we find that $\delta = 0.023 \pm 0.083$ ($\chi^2/DF = 0.1$) which is consistent with zero. If one uses the last four quark masses, then $\delta = 0.087 \pm 0.073$

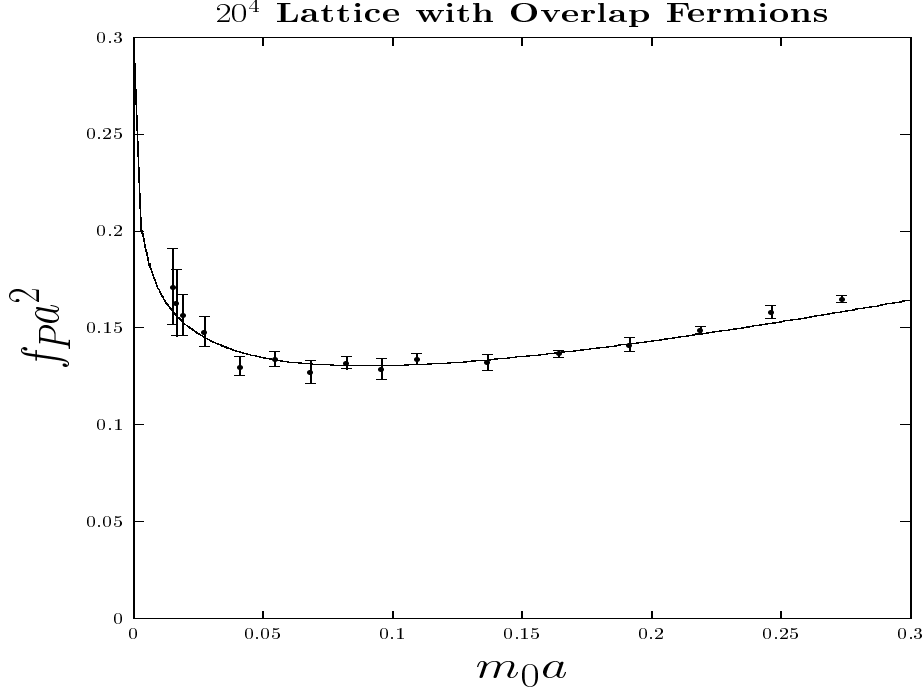


Figure 9: Renormalized $f_P a^2$ vs quark mass $m_0 a$. The solid line is a fit over the last 12 points with $\Lambda_\chi = 1.0$ GeV in Eq. (36).

$(\chi^2/DF = 0.02)$. Similar to the equal mass case, we cannot conclude that the chiral log exists from the masses of the pseudoscalar mesons with unequal quark masses from our data.

However, if we use more quark masses extending beyond $m_0 a = 0.1094$, the ratio becomes less than unity because m_{Pjj}^2 in the denominator deviates from the linear m_j dependence. This leads to a positive δ which is a false signal for the chiral log. This shows that one should be careful not to include in the ratio those masses which have a quadratic dependence on $m_0 a$.

Finally, we look for the chiral log in f_P , which according to Eq. (27) should grow in the form of $(\frac{1}{m_\pi^2})^\delta$. We calculate the renormalized f_P from

$$f_P = \lim_{t/a \gg 1} Z_P \sqrt{G_{PP}(t) 2m_P} e^{m_P t/2}, \quad (35)$$

where we insert the fitted m_P to obtain f_P . The renormalization constant Z_P is the same as the scalar renormalization constant Z_S . The latter is determined from the matching of renormalization group invariant quark masses at fixed pseudoscalar mass [8] and the details will be given elsewhere [35]. We plot the renormalized f_P in Fig. 9 as a function of m_π^2 . We see that it rises sharply at small quark mass and the $(\frac{1}{m_\pi^2})^\delta$ fit for the last 7 points give $\delta = 0.16(4)$ with $\chi^2/DF = 0.7$. However, the fit is limited in the sense that it cannot be extended to more data points due to the singular

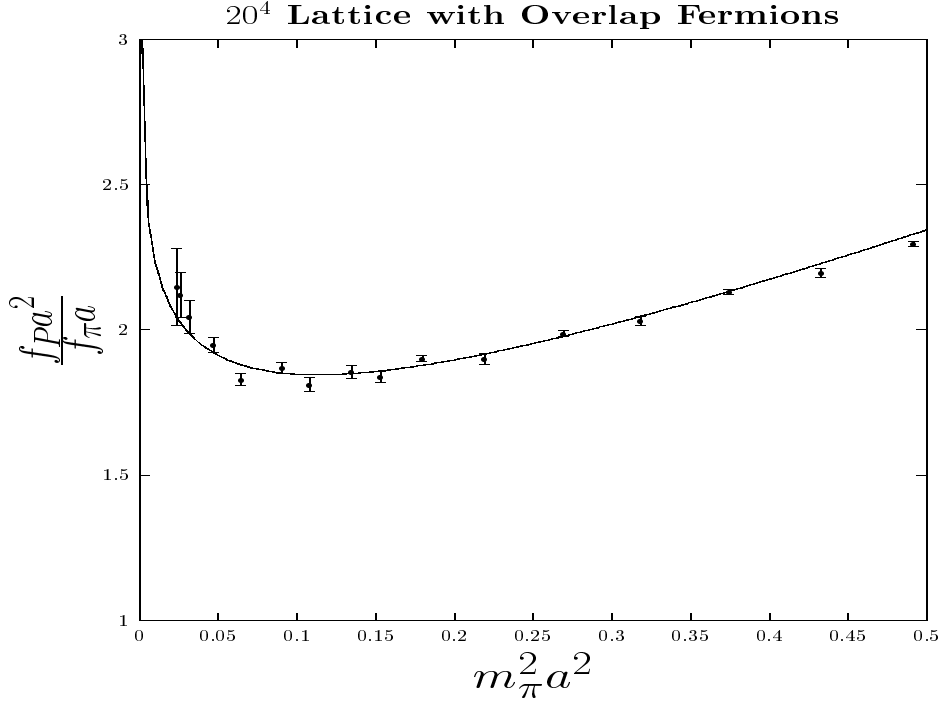


Figure 10: Renormalized $f_P a^2 / f_\pi a$ vs $m_\pi^2 a^2$. The solid line is a fit over the lowest 14 points.

nature of the fitting form. For example, fitting the last 8 points gives $\delta = 0.105(32)$ with $\chi^2/DF = 1.1$ which exceeds one. Since the log form in Eq. (30) falls off slower at larger quark mass, it might be better and may give a more stable fit covering a larger range of the quark mass. Based on this observation, we fit f_P in the log form

$$f_P a^2 = \tilde{f}_P a^2 \{1 - \delta[\ln(2Am_0/\Lambda_\chi^2) + 1]\} + Bm_0, \quad (36)$$

where we input A from the fit to m_P^2 in Eq. (30). Fits covering the range of 12 to 16 points and with Λ_χ from 0.6 GeV to 1.2 GeV give reasonably stable results. δ turns out to range from 0.2 to 0.4 and $\tilde{f}_P a^2$ ranges from 0.15 to 0.09. For the case of 12 points (up to $m_0 a = 0.1642$), $\delta = 0.199(50), 0.226(61), 0.252(76), 0.278(92)$ for $\Lambda_\chi = 0.6, 0.8, 1.0$, and 1.2 GeV respectively. $\tilde{f}_P a^2$ is between 0.1492(50) and 0.1071(78) in this case and $\chi^2/DF = 0.56$ in these fits. We see that δ obtained from either the log form or the power form is consistent with that predicted from the quenched η' loop in the chiral perturbation theory in Eq. (25) [28, 27]. We note that the general behavior of our data is close to what is observed in Ref. [27], but our δ is about three to five times larger than theirs.

To alleviate the apprehension that the apparent singular behavior of f_P may be caused by the boundary effect on the source in our lattice with fixed boundary

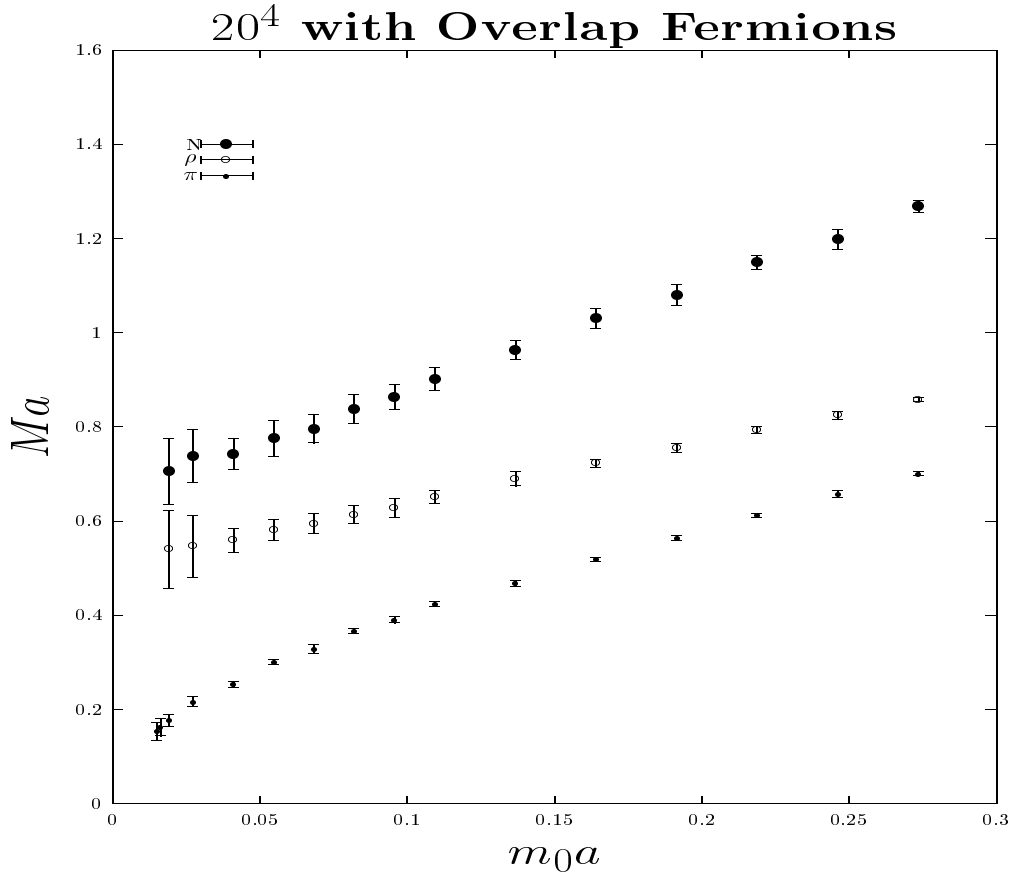


Figure 11: Nucleon, ρ and π masses vs quark mass m_0a .

condition, we consider the ratio of f_P in Eq. (35) and f_π in Eq. (19)

$$f_P a^2 / f_\pi a = \lim_{t \rightarrow \infty} \frac{Z_P \sqrt{2} m_P a G_{\partial_4 A_4 P}(\vec{p} = 0, t)}{2 m_0 a G_{A_4 P}(\vec{p} = 0, t)}. \quad (37)$$

This should cancel out the boundary effect on the source. We plot the ratio $f_P a^2 / f_\pi a$ as a function of $m_\pi^2 a^2$.

We see from Fig. 10 that the singular behavior is still visible in $f_P a^2 / f_\pi a$ which confirms that the chiral log singularity is indeed present in f_P . We fit them with the log form in terms of m_π^2

$$f_P a^2 / f_\pi a = A \{1.0 - \delta [\log(m_\pi^2 / \Lambda_\chi^2) + 1.0]\} + B m_\pi^2. \quad (38)$$

With $\Lambda_\chi = 1.0 \text{ GeV}$, we find that $\delta = 0.156(15), 0.181(22)$ and $0.217(36)$ for fits with 16, 14, and 12 points respectively. The χ^2/DF is 2.0 in these fits. We plot the fit with 14 points on Fig. 10 as the solid line.

6 Spectroscopy

We have also calculated ρ and nucleon masses in addition to the pseudoscalar masses. They are plotted in Fig. 11. With a fit of linear plus quadratic dependence on m_0a

for the last 12 points, we find $m_\rho a = 0.507(12)$ and $m_N a = 0.664(42)$ at the chiral limit with $\chi^2/DF = 0.02$ and 0.04 respectively. With $a = 0.157$ fm set from f_π , we find $m_\rho = 636(15)$ MeV which is 17% lower than the experimental value. Similarly, the nucleon mass $m_N = 833(54)$ MeV is 11% smaller than that of the experiment.

7 Summary

To conclude, we have studied the chiral properties of the pseudoscalar meson on a quenched lattice with overlap fermions. The lattice size is 20^4 with lattice spacing $a = 0.157$ fm set by the pion decay constant f_π . This gives a physical size of 3.14 fm which is about 3 times the Compton wavelength of the lowest mass pion.

We first clarified the role of the zero modes in the pseudoscalar meson propagator in association with the generalized Gell-Mann-Oakes-Renner relation. We find that the zero mode contribution to the pseudoscalar meson propagators extends to a fairly long distance in the time separation and it is imperative to avoid it since it is a finite volume effect. Otherwise, one might be led to wrong conclusions about the behavior of the pion mass and decay constants near the chiral limit. For example, if one fits the pion mass by choosing a time window which straddles over the kink in Fig. 2, one will find that the pion mass squared does not approach zero at the chiral limit with a linear extrapolation in the quark mass. Interpreting it as due to the quenched chiral log, one may fit it with a chiral log form and obtain a positive δ which can be misleading.

Due to the chiral symmetry of the overlap fermions, we obtain the non-perturbative renormalization constant Z_A from the axial Ward identity. The renormalized pion decay constant f_π is fairly constant over the mass range we consider which spans from about twice the average u and d mass to that of s . With a small error (1.6%) and devoid of the complication of the quenched chiral log, f_π is an ideal physical observable to set the scale of the lattice.

We studied extensively the issue of quenched chiral logs. Due to the limited statistics, we cannot tell if there are chiral logs in the pseudoscalar meson masses for both the equal and unequal quark mass cases. Due its singular nature, the quenched chiral divergence is finally seen clearly in $f_P a^2$. The fit to 12 points with the log form gives δ to be in the range of 0.2 to 0.3 which is quite in accord with that estimated from the double η propagator approximation of the quenched η' loop which predicts it to be ~ 0.18 .

The m_ρ and m_N at the chiral limit are 17% and 11% smaller than the experimental results which is to be expected in the quenched approximation.

We have finally have a reliable tool in the overlap fermions to study the chiral symmetry properties of hadrons at low energies including the quenched chiral logs.

One should go to different lattice spacings to study the continuum limit in the future.

This work is partially supported by DOE Grants DE-FG05-84ER40154 and DE-FG02-95ER40907.

References

- [1] For reviews, see for example, H. Neuberger, Nucl. Phys. **B (Proc. Suppl.) 83-84**, 67 (2000); F. Niedermayer, Nucl. Phys. **B 73**(Proc. Suppl.), 105 (1999).
- [2] H. Neuberger, Phys. Lett. **B 417**, 141 (1998).
- [3] R. Narayanan and H. Neuberger, Nucl. Phys. **B 443**, 305 (1995).
- [4] R.G. Edwards, U.M. Heller and R. Narayanan, Phys. Rev. **D 59**, 094510 (1999).
- [5] P. Hernández, K. Jansen, and L. Lellouch, Phys. Lett. **B469**, 198 (1999), [hep-lat/9907022].
- [6] T. DeGrand, hep-lat/0107014.
- [7] S.J. Dong, F.X. Lee, K.F. Liu, and J.B. Zhang, Phys. Rev. Lett. **85**, 5051 (2000), [hep-lat/0006004].
- [8] P. Hernandez, K. Jansen, L. Lellouch, and H. Wittig, hep-lat/0106011.
- [9] T. Degrand, hep-lat/0106001.
- [10] R.G. Edwards and U.M. Heller, Nucl. Phys. **94 (Proc. Suppl.)**, 737 (2001), [hep-lat/0010035].
- [11] C. Alexandrou, E. Follana, H. Panagopoulos, E. Vicari, Nucl. Phys. **B580**, 394 (2000), [hep-lat/0002010].
- [12] S. Capitani, Nucl.Phys. **B592**, 18 (2001), [hep-lat/0005008].
- [13] R.G. Edwards, U.M. Heller and R. Narayanan, Nucl. Phys. **B540**, 457 (1999).
- [14] R.G. Edwards, U.M. Heller and R. Narayanan, Phys. Rev. **D60**, 034502 (1999).
- [15] M. Lüscher and P. Weisz, Phys. Lett. **B 158**, 250 (1985); M. Alford, W. Dimm, and P. Lepage, Phys. Lett. **B 361**, 87 (1995).
- [16] K.F. Liu, S.J. Dong, F.X. Lee, and J.B. Zhang, Nucl. Phys. **B (Proc. Suppl.) 83-84**, 636 (2000).
- [17] C. Morningstar and M. Peardon, Phys. Rev. **D56**, 4043 (1997).

- [18] P. Hasenfratz, V. Laliena, and F. Niedermayer, Phys. Lett. **B427**, 125 (1998).
- [19] M. Lüscher, Phys. Lett. **B428**, 342 (1998), [hep-lat/9802011].
- [20] P. Chen et al., Nucl. Phys. **B (Proc. Suppl.) 73**, 207 (1999).
- [21] K.F. Liu, S.J. Dong, F.X. Lee, and J.B. Zhang, Nucl. Phys. **B (Proc. Suppl.) 83**, 636 (2000).
- [22] H. Leutwyler and A. Smilga, Phys. Rev. **D46**, 5607 (1992).
- [23] T. Blum et al., hep-lat/0007038.
- [24] K.F. Liu, S.J. Dong, F.X. Lee, and J.B. Zhang, Nucl. Phys. **B (Proc. Suppl.) 94**, 752 (2001), [hep-lat/0011072].
- [25] T. DeGrand, A. Hasenfratz, Phys. Rev. **D 64**, 034512 (2001), [hep-lat/0012021].
- [26] S.J. Dong, T. Draper, F.X. Lee, K.F. Liu, and J.B. Zhang, under preparation.
- [27] W. Bardeen, A. Duncan, E. Eichten, N. Isgur, and H. Thacker, hep-lat/0106008.
- [28] S. Sharpe, Phys. Rev. **D 46**, 3146 (1992).
- [29] G. Veneziano, Nucl. Phys. **B159**, 213 (1979).
- [30] K.F. Liu, Phys. Lett. **B281**, 141 (1992).
- [31] C. Bernard and M. Golterman, Phys. Rev. **D 46**, 853 (1992).
- [32] S. Aoki, et al., Phys. Rev. Lett. **84**, 238 (2000).
- [33] W. Bardeen, A. Duncan, E. Eichten, and H. Thacker, Phys. Rev. **D 62**, 114505 (2000).
- [34] J. Kiskis and R. Narayanan, hep-lat/0106018.
- [35] S.J. Dong, T. Draper, I. Horváth, F.X. Lee, K.F. Liu, and J.B. Zhang, under preparation.